SiF 2018– The 10th International Conference on Structures in Fire
FireSERT, Ulster University, Belfast, UK, June 6-8, 2018

FIRE PERFORMANCE OF LONG-SPAN COMPOSITE BEAMS WITH GRAVITY CONNECTIONS

Lisa Choe[1], Selvarajah Ramesh [2], Mina Seif[3], Matthew S. Hoehler[4], William Grosshandler [5], John Gross [6], Matthew Bundy [7]

ABSTRACT

Prescriptive fire-resistance ratings for structural components provide limited insight into the system-level performance of steel-concrete composite structures in fire. Specifically, long-span composite beam assemblies exposed to fire have vulnerabilities resulting from thermal restraint conditions that can be vastly different from those in short-span assemblies. This paper presents an overview of recent experiments on 12.8 m composite beams with various end support conditions, exposed to combined structural and fire loading. This paper focuses on the results for the specimens with double-angle beam-to-column connections, with and without slab continuity. The experiments showed that the specimens experienced similar thermal and displacement behaviour during the first 40 minutes after ignition regardless of the presence of slab continuity. The specimens exhibited local buckling of the beam near the connection, at the average bottom flange temperature of 400 °C. A thermal gradient in the specimen was observed during the heating and cooling phase. For the specimen with slab continuity, forces in the continuity bars increased when this local buckling occurred but decreased due to concrete fracture. This specimen did not collapse during the fire until its vertical displacement exceeded 1/20 span length. The collapse failure was observed during the cooling phase, which was resulted from weld fracture of the beam end connection due to contraction of the heated beam as it cooled down.

Keywords: Composite beams, double-angle connections, compartment fires, fire tests

1 INTRODUCTION

The span length of composite steel-concrete floor assemblies has increased over the years due to the availability of higher-strength materials, as well as architectural trends. The detailing of the member connections to withstand gravity loads (e.g., bolt hole and gap clearances), however, has

[1] Research Structural Engineer, National Institute of Standards and Technology, Gaithersburg, MD, USA.
e-mail: lisa.choe@nist.gov
[2] Guest Researcher, National Institute of Standards and Technology, Gaithersburg, MD, USA.
e-mail: selvarajah.ramesh@nist.gov
[3] Research Structural Engineer, National Institute of Standards and Technology, Gaithersburg, MD, USA.
e-mail: mina.seif@nist.gov
[4] Research Structural Engineer, National Institute of Standards and Technology, Gaithersburg, MD, USA.
e-mail: matthew.hoehler@nist.gov
[5] Guest Researcher, National Institute of Standards and Technology, Gaithersburg, MD, USA.
e-mail: william.grosshandler@nist.gov
[6] Guest Researcher, National Institute of Standards and Technolog, Gaithersburg, MD, USA.
e-mail: john.gross@nist.gov
[7] Supervisory Mechanical Engineer, National Institute of Standards and Technology, Gaithersburg, MD, USA.
e-mail: matthew.bundy@nist.gov

remained largely unchanged. Fire not only leads to degradation of material strength and stiffness, but also introduces additional forces into the assembly as thermal elongation is restrained by the adjoining structure. Since the magnitude of thermal strains is proportional to the heated length, the effect of thermal restraint is more significant on longer beams than shorter ones. These forces can potentially alter the sequence of failures in beam assemblies which are often only designed for limit states relevant to gravity loads at ambient temperature.

A series of 12.8 m composite beams exposed to combined structural and fire loading was recently conducted at the National Fire Research Laboratory [1]. This paper presents an overview of the test program, and the results for the specimens with double-angle connections. The goal of this work is to provide data to help advance performance-based fire design approach for steel frame buildings with composite floor systems.

2 TEST PROGRAM

2.1 Test Matrix and Specimen Design

Table 1 shows the test matrix. Test variables included the type of beam-end connections (double angles versus single plate) and the slab continuity conditions. Test 1 was an ambient-temperature test in which the ultimate moment capacity and the sequence of failure were studied [2]. The remaining specimens were subjected to flexural loading and fire. The applied flexural load was 45 % of the ultimate moment capacity (M_{max}) measured from Test 1. The fire was generated using three natural gas burners with a maximum total heat release rate of 4 MW.

The specimens were designed in accordance with current U.S. codes and standards [3, 4]. Details are presented in [5] and summarized here. *Fig. 1a* shows a cross-section of the specimens, which consisted of a 1.8 m wide by 12.8 m long concrete slab cast on trapezoidal metal decking, and a W18×35 floor beam. The slab was partially-composite with the steel beam via 19 mm headed shear studs spaced at 305 mm (design composite effectiveness 82 %). Welded wire fabric (0.06 mm^2/mm in orthogonal directions) was placed at the mid height of 83 mm thick concrete topping. The bottom flange of the beams with double-angle connections was coped at both ends. The steel beam was protected with Sprayed Fire Resistive Materials (SFRM) to achieve a 2 hour fire rating along the member and a 3 hour fire rating at the connections. *Fig. 1b* shows the specimen with the double-angle connections and slab continuity. The 9.5 mm thick angles were bolted to the beam web using three 19 mm high-strength structural bolts (with the minimum tensile strength of 830 MPa) and welded to a sacrificial plate on the flange of the column. The specimens for Test 3 and Test 5 included four no. 4 reinforcing bars (with the minimum tensile strength of 415 MPa) in the hogging moment region for crack control. Slab continuity was achieved by anchoring the reinforcement to a hollow steel section attached to the support column.

The steel beams and angles were made with hot-rolled steel with the minimum yield strength of 345 MPa and 250 MPa, respectively. The slab was cast using lightweight aggregate concrete with a design compressive cylinder strength of 28 MPa. The concrete mix included polypropylene microfibers to minimize spalling during heating. The measured ambient-temperature mechanical properties of all the structural components are reported in [5].

Table 1. Test Matrix

Test	Connection type	Slab continuity	Flexural load	Fire load
1	Double angle	No	M_{max}	
2	Double angle	No	$0.45M_{max}$	4 MW
3	Double angle	Yes	$0.45M_{max}$	4 MW
4	Single plate	No	$0.45M_{max}$	4 MW
5	Single plate	Yes	$0.45M_{max}$	4 MW

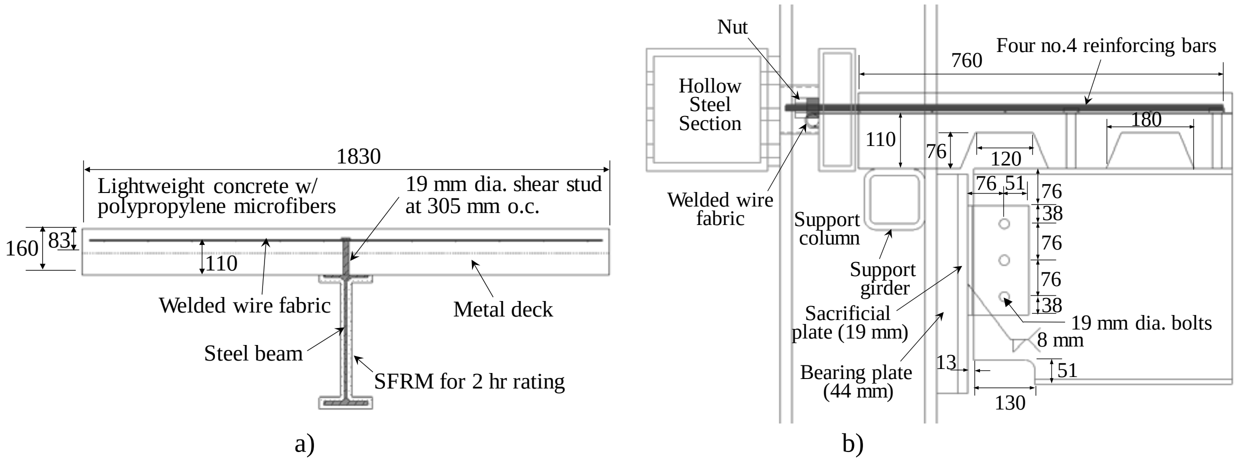

Fig. 1. a) Cross section of the specimen; b) Connections of specimen with double-angles and continuity (units: mm)

2.2 Test Setup, Fire Load, and Instrumentation

The test setup is shown in *Figs. 2a* and *2b*. The composite beam specimen was supported by W12×106 columns with bracing modules, using the connections listed in *Table 1*. The distance from the center bolt of the beam connection to the strong floor was 3.6 m. The measured average lateral stiffness of the braced column at this height (i.e. the axial stiffness provided at the beam ends) was 220 kN/mm. The beam specimen was loaded by six equally distributed point loads (*Fig. 2a*). Three loading beams running transverse to the specimen were loaded using an actuator at each of the six ends. The vertical force of each loading beam was transferred to the beam specimen via triangular trusses. The slab was laterally braced at the locations of the three loading beams. The vertical displacements and end rotations of the specimen were measured using four linear position transducers and two inclinometers mounted on the top of the slab, respectively. The thermally-induced axial restraint force at the beam support was measured using the strain gauges attached on the diagonal brace members of the bracing modules. Washer load cells were used to measure the forces in the no. 4 reinforcing bars in Tests 3 and Test 5.

Three natural gas burners (each 1 m wide × 1.5 m long) distributed along the center of the compartment floor were used to heat the specimen. The fire was designed to achieve an upper layer temperature of around 1000 ºC, and avoid combustion outside of the compartment. Peak heat release rate per unit volume was 40 kW/m^3, which corresponds to a range of total fuel loads between 550 MJ/m^2 and 1100 MJ/m^2 for fire durations between one and two hours. To confine the fire below the specimen, enclosure walls (with a total surface area of 110 m^2) were constructed using cold-formed steel framing and sheet steel as shown in *Fig. 2b*. The total ventilation opening area was about 5 m^2. The fire-exposed wall surfaces were protected with a 50 mm thick layer of ceramic blankets. *Fig. 2c* shows the predicted spatially-averaged temperatures in the upper gas layer and along the lower flange of the steel beam underneath the SFRM layer, using the Fire Dynamic Simulator (FDS) [6] prior to conducting the test series. The heat release rate increases linearly to a maximum of 4 MW during the first 15 minutes and remains steady up to 70 minutes, followed by a linear decrease to zero at 112 minutes.

Fig. 3 show the thermocouple layout. Four Inconel shielded thermocouples (K-type, 24 gauge) were used to measure the average bottom flange temperature. Glass-sheathed thermocouples were mounted at various locations of the steel beam and the connection elements. However, there was considerable difficulty in getting reliable temperatures of the steel beam beyond the first fifteen minutes of the heating. Glass shielding of thermocouples burned off and made secondary junctions when exposed to hot gas temperatures. In some cases, contact between the thermocouple beads and the steel surface could not be maintained as the beam heated and deformed. In other cases, fissures in the insulation layer permitted hot gas to penetrate to the thermocouple on steel surface. All these effects could lead to higher temperature readings during heating. *Table 2* summarizes the estimated total expanded measurement uncertainties with a coverage factor of 2 as defined in [7].

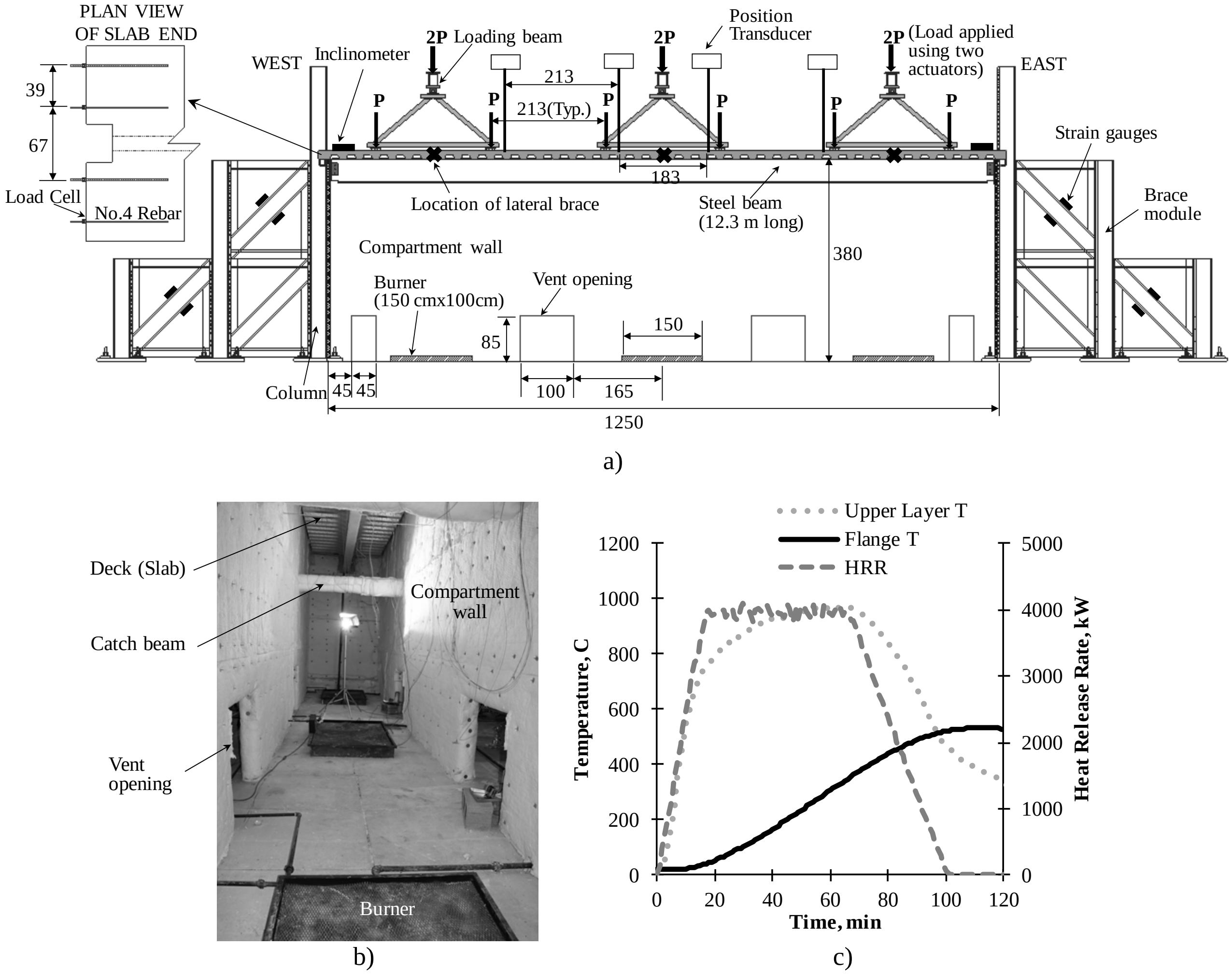

Fig. 2. a) Longitudinal section of the setup (units: cm); b) Photograph of inside the compartment; c) Temperature predictions using the FDS

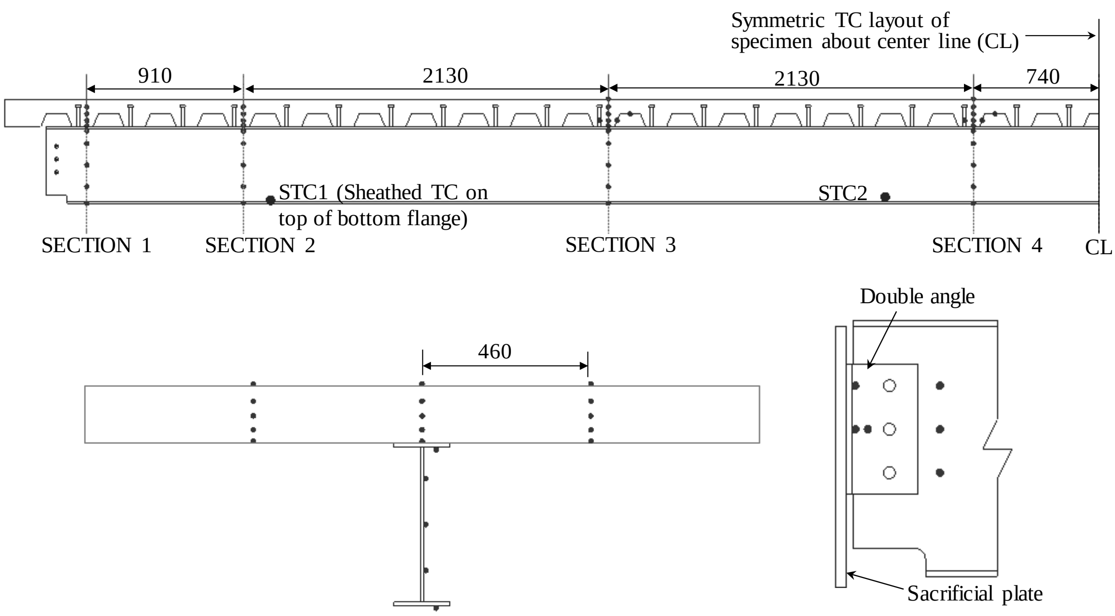

Fig. 3. Location of thermocouples along the beam length, in the beam cross section and connection region (units: mm)

Table 2. Measurement Uncertainty

Measurand	Range (max)	Total expanded uncertainty (coverage factor of 2)
Mechanical load (Actuators)	220 kN	±10 %
Displacement	760 mm	±15 %
Strain	50,000 με	±6 %
Heat release rate	4 MW	±7 %
Steel Temperature (Inconel sheathed thermocouples)	1200 °C	±25 %

3 RESULTS AND DISCUSSION

Tests 2 (T2) and Test 3 (T3) studied the behaviour of the composite beam with the double-angle connection subjected to combined flexural loading and compartment fire described above. The experiments were conducted as follows: i) A total mechanical load of 106 kN was applied and held constant at ambient temperature, ii) the heat release rate was increased to 4 MW over a period of 15 minutes and held constant until the mechanical load was eliminated, and iii) the cooling phase was initiated by linearly decreasing the heat release rate over 30 minutes.

Fig. 4a shows plots of the total mechanical load and the burner heat release rate. *Fig. 4b* shows the average gas temperature measured using thermocouple probes located 810 mm below the slab and the heat release rate measured with the calorimeter. Elimination of the mechanical loads was triggered by the pre-set limit of actuators. In Test 2, the actuators were depressurized when the total mechanical load dropped below 90 kN (about 85 % of its original value applied at ambient temperature) around 30 minutes, when the beam web near the angle connection buckled.

For Test 3, the pre-set load limit was removed and a displacement limit was implemented instead. The mechanical load was removed around 65 minutes after ignition when the vertical displacement of the specimen reached 620 mm. The heat release rates and resulting gas temperatures were comparable until 40 minutes (*Fig. 4b*). The gas temperature reached 900 °C at 15 minutes after ignition. Peak average temperatures exceeded 1000 °C around 40 minutes. The maximum measured temperatures were as much as 100 °C above the values predicted by FDS model (*Fig. 2c*).

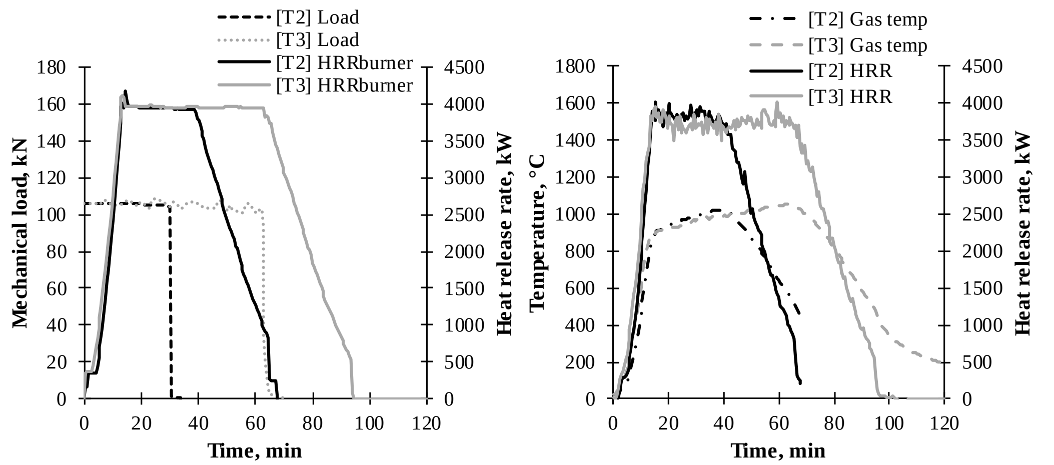

a) b)

Fig. 4. a) Heat release rate based on fuel flow and total mechanical load applied using actuators; b) Heat release rate measured using the calorimeter and gas temperature inside the compartment

3.1 Thermal Response

Fig. 5 shows the range of a) the average steel temperatures at various locations, including the bottom flange of the steel beam in the middle of compartment and the connection region, and b) the slab temperatures near midspan. Since similar fire conditions were maintained in Tests 2 and 3 up to 40 minutes (*Fig. 4*), the thermal response of the specimens for these tests was comparable.

Although the upper layer gas temperature was approximately constant with an average standard deviation of 30 °C, a thermal gradient still existed in the specimen along the beam length and across the section. The metal deck rapidly heated with increasing gas temperatures, exceeding 700 °C in 1 hour after ignition. The temperature increase in the connection region with thicker SFRM and inside the slab above the steel beam was slower. In Test 3, the measured peak average temperature of the beam web next to the edges of the angle and the angle itself were around 400 °C and 200 °C, respectively. The temperatures in the slab above the steel beam remained below 300 °C.

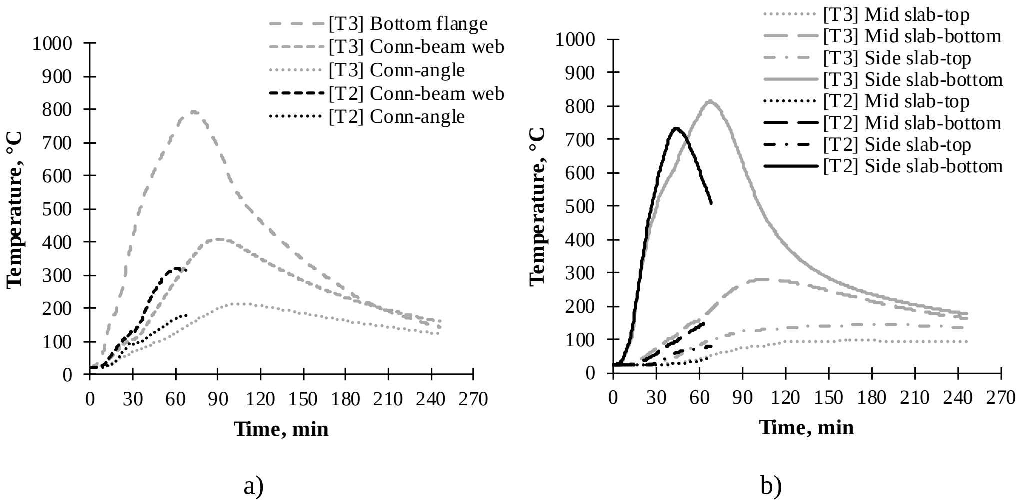

Fig. 5. a) Steel temperatures; b) Concrete temperatures measured in Test 2 and 3

3.2 Structural Response and Failure

The specimens with the double-angle connections exhibited diverse behaviours during the heating and cooling. *Fig. 6* shows the vertical displacement of the specimen measured 1.1 m from midspan and the average axial restraints induced at the beam ends as a function of the beam lower flange temperature. The positive values of displacements indicate downward displacements; the negative values of axial restraints represent compressive axial force in the specimen.

As shown in *Fig. 6a*, for both Tests 2 and 3, the specimen deflected downward after ignition. The beam web near the angle connection buckled around 30 minutes, at the corresponding bottom flange temperature of 400 °C. The peak axial restraint of 370 kN was observed around this temperature (*Fig. 6b*). From this point through the cooling phase, there was no further failure observed in Test 2 since the mechanical load was removed. During the 30-minute period at which the heat release rate linearly decreased, the vertical displacement continued to increase due to the weight of the specimen and loading fixtures. For Test 3, in which this pre-set load limit was eliminated, the loaded specimen continuously bent down with increasing temperatures following buckling of the beam web around 400 °C. The mechanical load was removed at the vertical displacement of 620 mm (1/20 span length), at the bottom flange temperature of 760 °C. The heated specimen continued to deflect downward while the heat release rate was decreased. The measured peak vertical displacement was 690 mm (1/18 span length). The vertical displacement decreased after the burner was shut off. *Figs 6c-d* show photographs of the specimens after cool-down.

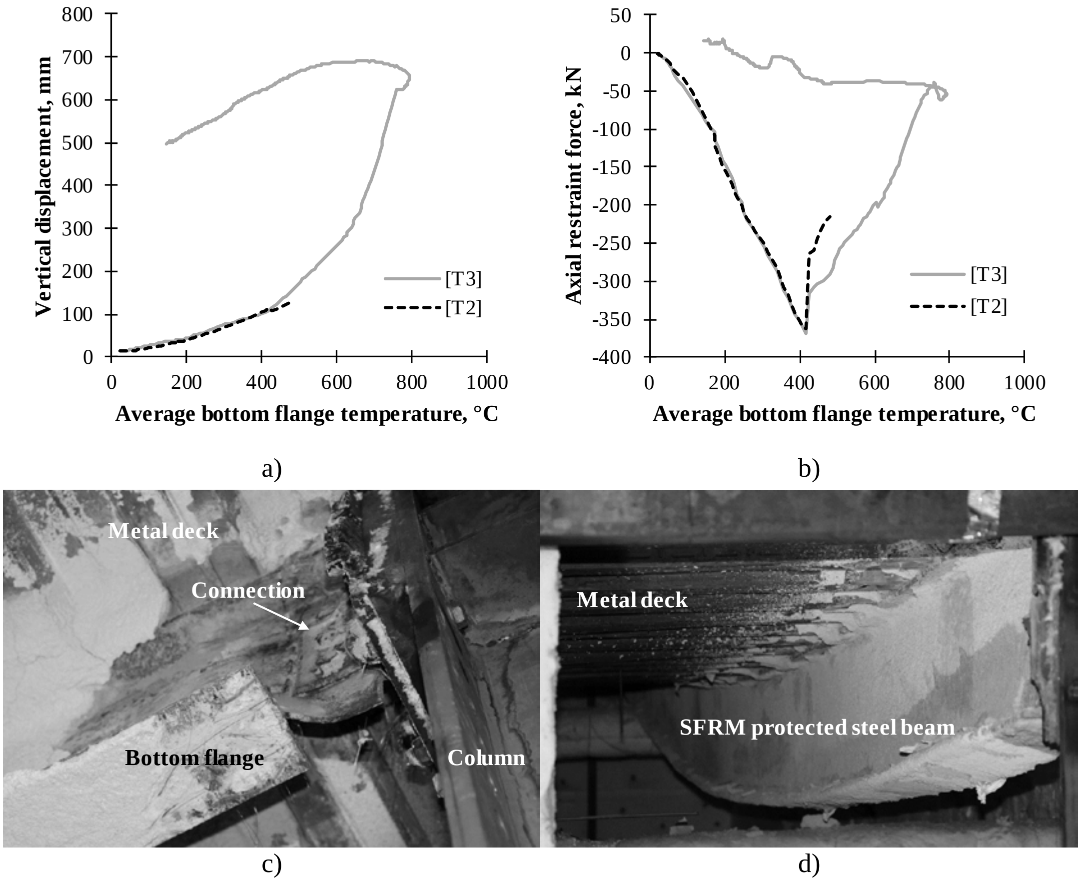

Fig. 6. a) Vertical displacement; b) Axial restraint force as a function of average bottom flange temperature; c-d) Photograph of buckled beam web (Test 2) and deformed specimen (Test 3) after cool-down

The concrete slab in Test 3 had no. 4 reinforcing bars anchored at slab ends (*Fig. 1*). *Fig. 7a* shows a comparison of the tensile forces developed in the bars, located at 335 mm from the longitudinal centreline of the slab (*Fig. 2a*), along with the range of the vertical displacement of the specimen. *Fig. 7b* shows a photograph of fracture after the test. The tensile forces in the rebars significantly increased after buckling of the beam web occurred around 30 minutes. The magnitude of tensile forces became larger as the vertical displacements increased from 200 mm to 350 mm, followed by a rapid drop indicating the development of concrete failure near the reinforcement. The triangular shape of concrete fracture was observed after cool-down, as shown in *Fig. 7b*.

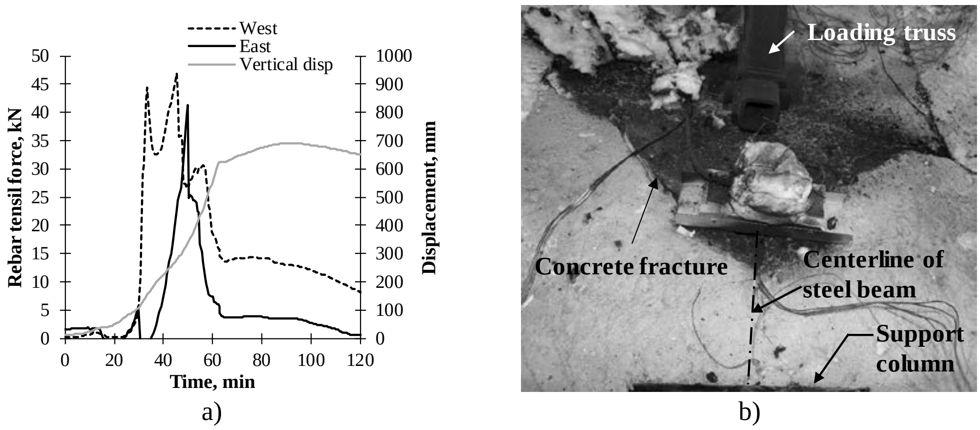

Fig. 7. a) Forces in the continuity bars; b) Slab at west end after cool-down

This specimen did not collapse during the fire. Around five hours after the fire was extinguished, however, the specimen collapsed by weld fracture of the east angle connection. The angles at both ends pried due to contraction of the specimen during cool-down, but there was neither weld failure of the west angle connection nor failure of shear studs.

4 CONCLUSIONS

The fire experiments on the loaded steel-concrete composite beam specimens with double-angle connections (Tests 2 and 3) showed:

- Similar thermal and structural responses during the first 40 minutes after ignition;
- A thermal gradient along the beam length and across the section during the heating and cooling phase in Test 3;
- Local buckling of the beam near the connection and increase of tensile forces in the continuity bars around 30 minutes after ignition, at the average bottom flange temperature of 400 °C;
- Vertical displacements exceeding 1/20 times the span length during the fire in Test 3; and
- Collapse failure by weld fracture of the double angle connection at east end during the cooling phase in Test 3.

ACKNOWLEDGMENTS

The authors would like to acknowledge the great support of NIST colleagues for their hard work to safely complete the experiments. They would also like to thank the expert panel members including William Baker, Glenn Bell, Craig Beyler, Luke Bisby, Ian Burgess, Charlie Carter, Charles Clifton, Michael Engelhardt, Graeme Flint, Nestor Iwankiw, Kevin LaMalva, Roberto Leon, Jose Torero, and Amit Varma for their support throughout this project.

REFERENCES

1. Bundy, M., Hamins, A., Gross, J., Grosshandler, W., and Choe, L. (2016). *Structural fire experimental capabilities at the NIST National Fire Research Laboratory*. Fire Technology, 52(4), 959-966.
2. Choe, L., Ramesh, S., Hoehler, M., Gross, J. (2018). Experimental Study on Long-Span Composite Floor Beams Subject to Fire: Baseline Data at Ambient Temperature. *Proc. of Structures Congress 2018*, Fort Worth, Texas, April 19-21, 2018.
3. ANSI/AISC-360 (2016). *Specificication for Structural Steel Buildings*. American Institute of Steel Construction, Chicago, Illinois.
4. ASCE/SEI 7 (2016). *Minimum Design Loads for Buildings and Other Structures*. American Society of Civil Engineers, Reston, Virginia.
5. Ramesh, S., Choe, L., Hoehler, M., Grosshandler, W., Gross, J. (2018). Design and Construction of Long-Span Composite Beam Specimens for Large Structural-Fire Tests. *Proc. of Structures Congress 2018*, Forth Worth, Texas, April 19-21, 2018.
6. McGrattan, K., Hostikka, S., McDermott, R., Floyd, J., Weinschenk, C., and Overholt, K. (2013). Fire Dynamics Simulator, Technical Reference Guide, National Institute of Standards and Technology, Gaithersburg, Maryland, USA, and VTT Technical Research Centre of Finland, Espoo, Finland, sixth edition, September 2013.
7. Taylor, B. N., and Kuyatt, C. E. (1994). *Guidelines for Evaluating and Expressing the Uncertainty of NIST Measurement Results*. National Institute of Standards and Technology, NIST Technical Note TN-1297, Gaithersburg, Maryland.